

Transmission characteristics of a two-dimensional photonic crystal array of dielectric spheres using subterahertz time domain spectroscopy

T. Kondo* and M. Hangyo

Research Center for Superconductor Photonics, Osaka University, 2-1 Yamadaoka, Suita, Osaka 565-0871, Japan

S. Yamaguchi

Graduate School of Science and Technology, Chiba University, 1-33 Yayoi-cho, Inage-ku, Chiba 263-8522, Japan

S. Yano and Y. Segawa

Photodynamics Research Center, The Institute of Physical and Chemical Research (RIKEN), 519-1399 Aoba, Aramaki, Aoba-ku, Sendai, Miyagi 980-0845, Japan

K. Ohtaka

Center for Frontier Science, Chiba University, 1-33 Yayoi-cho, Inage-ku, Chiba 263-8522, Japan

(Received 8 February 2002; published 31 July 2002)

The transmission characteristics of a two-dimensional millimeter-sized Si_3N_4 sphere array system are measured and compared with calculations. The transmittance and the phase shift are measured by the subterahertz time domain spectroscopy and the calculation is based on the vector KKR formalism. Excellent agreement over a wide frequency range for the transmittance, phase shift, and photonic band structure has been obtained. The results show that, provided the system is well prepared geometrically and absorption can be suppressed, periodic arrays of dielectric spheres are very promising as photonic crystals.

DOI: 10.1103/PhysRevB.66.033111

PACS number(s): 42.70.Qs, 78.47.+p, 42.25.Bs

A periodic array of dielectric spheres or a dielectric material with a periodic array of spherical voids is a prototypical photonic crystal, and demonstrates the basic physics of photonic crystals of more sophisticated fabrication.¹⁻³ As to the theory of the dielectric sphere array systems, methods for calculating various properties with high accuracy based on the vector KKR formalism have been developed by one of the authors.⁴ However, theory and experiment have not been adequately compared because of the insufficient uniformity of the size of the spheres and the imperfect lattice stacking of samples, except for a recent study on a opal made of 855-nm silica spheres.⁵ Obviously better photonic crystals composed of sub-micrometer-sized spheres, which are technologically exploitable, should be prepared.⁶⁻¹⁰

Arrays of dielectric spheres are valuable in studying the physics of the photonic band, based on a tight-binding model of electrons in crystals. A photon in an isolated dielectric sphere experiences an attractive potential and is easily confined within the sphere, like an electron bound to an atom. In a regular array of dielectric spheres, the confined photon can hop from one sphere to its neighbor by the optical tunnel effect. The coherent motion of the photon in the periodic lattice of dielectric spheres gives rise to a photonic band specified by a wave vector k . Therefore, the photonic band in the array of dielectric spheres reflects the original character of a localized state as in the electronic bands in insulating crystals. This is the basis of photonic bands in an array of dielectric spheres.

It is important to understand the properties of the two-dimensional (2D) systems since the real photonic crystals for applications are made for a slab crystal with a thickness of a few or several periodicities, which are governed in many ways by the 2D properties of photonic bands rather than

those of 3D ones. The photonic bands within the light cone in k - ω space (where ω is the angular frequency) are in general leaky and have a finite lifetime. This is because confinement is incomplete due to the finite array size in the direction perpendicular to the array plane. To specify the lifetime, it is then necessary to solve Maxwell equations taking into account the photonic bands coupled with the plane-wave states of the exterior region. The following analysis is based on an exact treatment of such mixing effects.

In this paper, we show how well a sphere array can reproduce theoretical predictions. Millimeter-sized Si_3N_4 spheres are arrayed in a 2D triangle lattice and examined. The transmission characteristics of the 2D sphere array system are measured using sub-terahertz (sub-THz) time domain spectroscopy (TDS),¹¹⁻¹³ and compared with calculations based on the vector KKR formalism.¹⁴ Excellent agreement is obtained over a wide frequency range for the transmittance, phase shift, and photonic band structure.

A 2D array of Si_3N_4 spherical balls with a diameter d of 1/8 in. ($=3.175$ mm) was set up. These spheres are known to be accurately spherical shape and uniform size, with a variation in diameter of less than 1/2000 in. ($=0.0127$ mm). The Si_3N_4 spheres were manually placed on the xy plane in a monolayer triangle lattice, with a lattice constant $d=3.175$ mm in a 50-mm \times 42-mm-sized aluminum frame. Both faces of the resulting 2D photonic crystal were fixed by 55- μm -thick vinyl films. The complex amplitude of the wave transmitted directly through this system was measured over a very wide frequency range by sub-THz TDS (Refs. 11-13) in the atmosphere. The power transmittance and the phase shift spectra were obtained simultaneously, in the frequency range ~ 30 to ~ 300 GHz, from the two sub-THz waveforms in the time domain. The first is

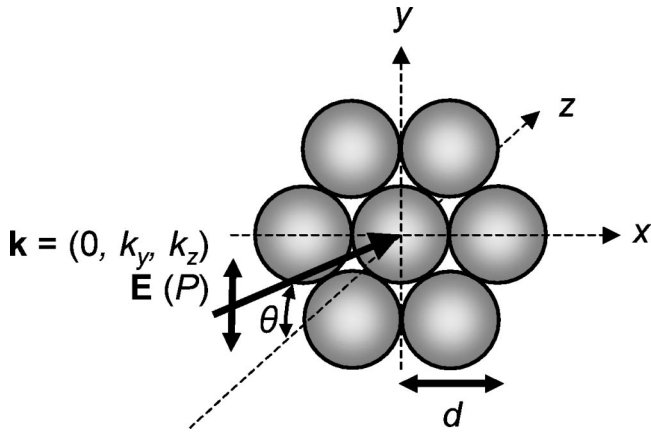


FIG. 1. Experimental configuration.

denoted by $E_{\text{sam}}(t)$, and is obtained by placing the sample in the sub-THz beam path; the second is the reference sub-THz waveform $E_{\text{ref}}(t)$ measured without the sample. By taking the Fourier transform of these $E(t)$, we can obtain the complex amplitude spectrum having magnitude $|E(\omega)|$ and phase $\phi(\omega)$ in the form $E(\omega) = |E(\omega)|\exp[i\phi(\omega)]$. The power transmittance $T(\omega)$ and the phase shift $\Delta\phi(\omega)$ of the sample are then given by

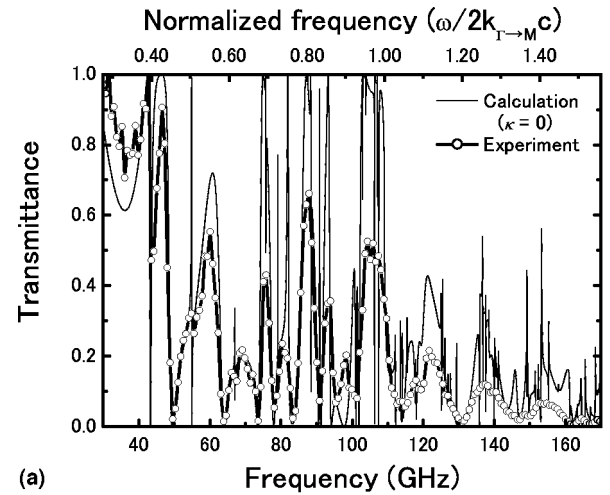
$$T(\omega) = |E_{\text{sam}}(\omega)|^2 / |E_{\text{ref}}(\omega)|^2, \quad (1)$$

$$\Delta\phi(\omega) = \phi_{\text{sam}}(\omega) - \phi_{\text{ref}}(\omega). \quad (2)$$

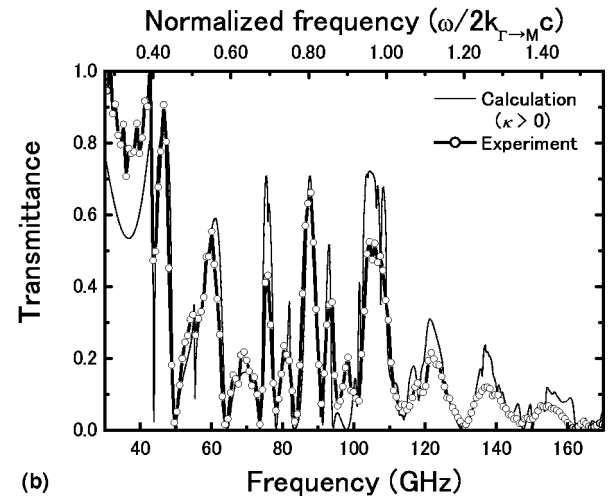
The incident wave was a p -polarized sub-THz wave emitted by a bow-tie-shaped low-temperature-grown GaAs photoconductive antenna (LT-GaAs antenna).^{12,13} It impinges on the sample at an incidence angle θ , as shown in Fig. 1. The 2D wave vector $\mathbf{k} = (0, k_y, k_z)$ of the incident wave is set up along the symmetry axis Γ -M of the 2D Brillouin zone. The distance between the points Γ and M is $|\mathbf{k}_{\Gamma \rightarrow \text{M}}| = 2\pi/d\sqrt{3}$. The transmitted p -polarized wave was detected by a bow-tie-shaped LT-GaAs antenna. The spot size of the incident beam on the sample was about 40 mm in diameter, and the frequency resolution of this measurement system was estimated to be 0.75 GHz. The illuminated area contains about 200 spheres and the finite size effect can be neglected.

Figure 2(a) shows the measured and calculated transmission spectra at an incidence angle $\theta = 0^\circ$ (normal incidence). In this case, first-order Bragg diffraction occurs at 109.1 GHz. The theoretical transmittance was calculated using the vector KKR method.¹⁴ In this calculation the refractive index of Si_3N_4 is taken as $n = 2.99$ and its imaginary part is neglected. The lattice constant d is the only other parameter used in the calculation.

The measured spectrum shows a number of distinct dips. This fine structure will be shown to be due to excitation of the optically active 2D photonic band, meaning a band that is coupled to the external light. Figure 2(a) shows that the overall pattern of the observations agrees well with the calculation. Agreement is particularly good in the range 40–75 GHz. However, the absolute value of the calculated transmittance is larger than that found experimentally. Furthermore, some of the asymmetric spiky features accompanied by rapid



(a)



(b)

FIG. 2. Experimental transmission spectrum of the Si_3N_4 sphere array system at normal incidence compared with the calculated result. Circles with solid line represent data obtained by TDS with a resolution of 0.75 GHz. The fine solid line represents the calculated result (a) with $n = 2.99$, $\kappa = 0$ and (b) with $\kappa > 0$ (Ref. 16).

falls to zero in the calculation, which are characteristic of the Fano effect,¹⁵ are absent in the experimental results.

Figure 2(b) shows the transmission spectrum, which is calculated by allowing for the absorption of Si_3N_4 and the transmittance of the thin vinyl films. The experimental data of Fig. 2(a) are also reproduced. From the experimental transmission data for a 3.95-mm-thick plate sample of Si_3N_4 using TDS, we found that the complex refractive index $[n(\omega), \kappa(\omega)]$ of Si_3N_4 shows weak dispersion in the frequency region examined, varying from (2.96, 0.0038) at 50 GHz to (2.99, 0.0054) at 100 GHz. To obtain the theoretical result of Fig. 2(b), the complex refractive index was fitted by a third-order polynomial in ω .¹⁶ The transmittance of the thin vinyl films was measured to be 93% in the sub-THz frequency range. We multiply the calculated transmittance by $(0.93)^2$ to take account of the two films. The interference effect between the two films and the photonic crystal can be neglected because of the low reflectivity of the films. Compared to the calculated curve of Fig. 2(a), the magnitude of the transmittance is much reduced, and many spiky struc-

tures disappear. As a result, agreement is greatly improved across a wide frequency region. Agreement is especially close in the low frequency region below 95 GHz. This implies that the photonic crystal used in this study has an ideal lattice and good uniformity in the size of spheres, and that absorption by Si_3N_4 is mainly responsible for the discrepancy between the experiment and theory seen in Fig. 2(a). The importance of the absorption coefficient for interpreting the transmission spectra of photonic crystals has been pointed out by Hase *et al.* at first for a 2D photonic crystal made of dielectric rods.¹⁷ Close agreement over a wide frequency range covering so many photonic bands, presented here, has not been reported previously.

The phase of the complex transmission amplitude is also important, since it carries information about the density of states of photonic bands. The measurement of the phase shift spectrum and a comparison with theory has not previously received much attention except in Ref. 14. The differential of the phase shift with respect to frequency gives the density of states of the photonic bands of the slab, which we refer to as the optical density of states (ODOS),¹⁴

$$\text{ODOS}(\omega) = \frac{1}{\pi} \frac{\partial}{\partial \omega} \Delta \phi(\omega). \quad (3)$$

The lifetime of leaky photonic bands is inversely proportional to the full width at half maximum (FWHM) of the Lorentzian peak in the ODOS.¹⁴ As mentioned above, the reliable phase shift spectrum is also measured by TDS.¹¹⁻¹³ The phase shift $\Delta \phi(\omega)$ is given by

$$\Delta \phi(\omega) = \Delta \phi_0(\omega) + 2\pi j \quad (j=0, \pm 1, \pm 2, \dots), \quad (4)$$

where $\Delta \phi_0(\omega)$ is the principal value of the phase shift, which is the quantity obtained directly by the measurement and calculation.¹⁸

Figure 3 shows the phase shift spectra at normal incidence ($\theta=0^\circ$). The calculated curve with $\kappa=0$ shows a number of steps in $\Delta \phi(\omega)$, each revealing the presence of a leaky photonic band through the ODOS peaks that follow from Eq. (3). Although the calculated phase shift, the integrated ODOS, increases monotonically, as expected, the experimental value decreases in such frequency regions (marked by arrows in Fig. 3). This is attributed to the absorption; we recalculated the phase shift by taking account of the nonzero absorption¹⁶ and obtained better agreement, as shown in Fig. 3. The agreement between experiment and theory has been greatly improved compared to the previous report,¹⁴ in which the measurement of the phase shift by the vector network analyzer had a large ambiguity and the calculation did not take into account the absorption by the Si_3N_4 material.

The incident angle dependence of the transmittance and the phase shift spectra provide the dispersion relation of 2D photonic bands. For the angle of incidence θ , the wave vector \mathbf{k} of the photonic bands excited in the system is given by

$$k = \frac{\omega}{c} \sin \theta, \quad (5)$$

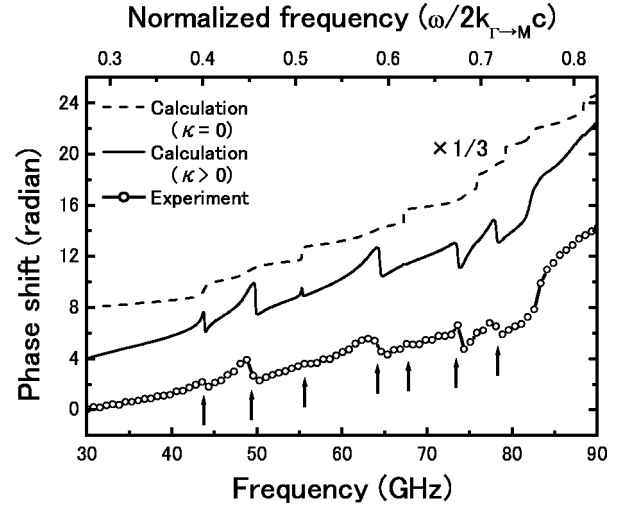


FIG. 3. Experimental phase shift spectrum compared with calculated values. Dashed and solid lines, respectively, represent the calculated result for $n=2.99$ and $\kappa=0$, and taking into account the absorption (Ref. 16). Circles with solid line represent data measured by TDS. Arrows show the positions of the leaky modes seen experimentally. For ease of comparison, the two phase shift curves are given a vertical offset of 4 rad.

where c is the light velocity in free space. The analysis of Ref. 14 indicates that photonic bands show up mostly as dips in the transmission spectra.¹⁹ Correspondingly, we take the dips in the transmission spectra to indicate the existence of 2D photonic bands, and plot these as θ varies with steps of 3° up to 30° to obtain the experimental dispersion relation for the 2D photonic bands. Figure 4 shows the observed band dispersions of the p -polarization-active photonic bands. The open circles and the accompanying bars show the dip positions in the transmission spectra and the FWHM of the sharp

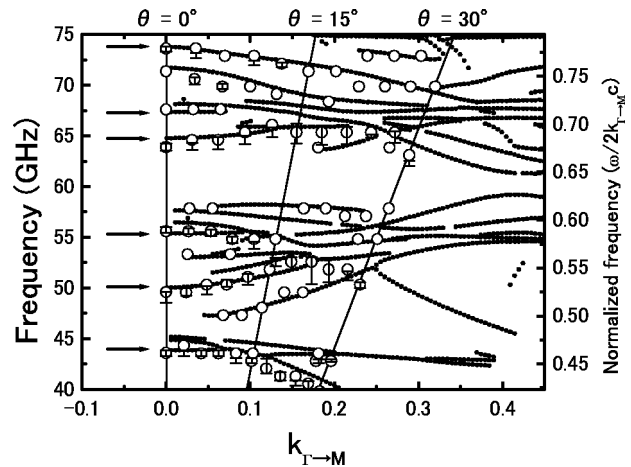


FIG. 4. Experimental and theoretical dispersion curves of 2D photonic bands responsive to the p -polarized sub-THz wave. The horizontal axis is normalized so that $k_x=0.5$ at the M point of the first Brillouin zone. Solid circles are the theoretical dispersion curves, and open circles are the measured values. The bars on the data points show the measured FWHM. The three straight lines are the k - ω curves given by Eq. (5).

peaks obtained from the measured phase shift of Fig. 3, respectively. For dips with the FWHM larger than 3 GHz, we do not show the bars. Also shown, as lines made up of solid circles, are the theoretical dispersion relations obtained from the dip position of the transmission spectrum, calculated for $\kappa > 0$.¹⁶ Figure 4 demonstrates a good agreement between theory and experiment, including the photonic bands located in the higher frequency region. This verifies that many photonic bands are excited in the experiment. In particular on the photonic bands marked by the solid arrows, which appear as distinct dips in the transmittance at the Γ point ($\mathbf{k}=0$), the theoretical dispersion curves are followed accurately by the transmittance experiment throughout the Brillouin zone (see, e.g., Refs. 20 and 21 for the group-theoretical analysis of the optical activity).

The bands that did not respond to the incident light at the Γ point were more difficult to observe. With increasing k , leakage begins and these bands gradually become optically active. However, in the range of $\theta < 30^\circ$ examined here, the coupling with the external light is not strong enough to survive the absorption effect. These modes are therefore demolished by absorption before they are able to couple fully with the external light. Consequently, in spite of the presence of many unrecognizable photonic bands in Fig. 4, the discrepancy between theory and experiment in the line shape of the optical response is small.

In summary, we have demonstrated the best agreement yet between experiment and theory for photonic crystals of spheres. Millimeter-sized photonic crystals of spheres will be technologically useful as filters, resonators, waveguides, etc.

in communications and in imaging with millimeter waves. They are also useful as a test of the performance of photonic crystals of smaller lattice constant, because we can make use of the scaling rule for the wavelength of light and the periodicity of the lattice. The present results therefore provide a useful guide to the quality of the array of spheres needed for use in the visible and infrared regions.^{6–10} Through the enhanced Q values following from the good confinement effect of “gallery modes” of spheres, theory verifies that the narrow photonic bands in a photonic crystal made of spheres reduce the lasing threshold,²² enhance the near-field intensity,²³ and enhance resonant Smith-Purcell radiation.²⁴ Improvement in the predicted performances is by orders of magnitude. We have demonstrated that, provided the system is well prepared geometrically and absorption can be suppressed, periodic arrays of dielectric spheres are very promising as photonic crystals.

We thank Dr. S. Nashima for technical assistance and Professor M. Tonouchi for his encouragement. We are grateful to Dr. H. Miyazaki at National Institute for Materials Science for informing us Ref. 17. This work was supported by a Grant-in-Aid for a Specific Scientific Area and a “Promotion of Science” grant from the Ministry of Education, Culture, Sports, Science, and Technology of Japan. T. and M. acknowledge support by the public participation program for the promotion of creative info-communications technology R&D of the Telecommunications Advanced Organization of Japan (TAO). T. also acknowledges the Japan Society for the Promotion of Science.

*Electronic address: kondo@rcsuper.osaka-u.ac.jp

¹K. Ohtaka, Phys. Rev. B **19**, 5057 (1979).

²E. Yablonovitch, Phys. Rev. Lett. **58**, 2059 (1987).

³S. John, Phys. Rev. Lett. **58**, 2486 (1987).

⁴K. Ohtaka and Y. Tanabe, J. Phys. Soc. Jpn. **65**, 2265 (1996).

⁵Y.A. Vlasov, X.-Z. Bo, J.C. Sturm, and D.J. Norris, Nature (London) **414**, 289 (2001).

⁶A. van Blaaderen, R. Ruel, and P. Wiltzius, Nature (London) **385**, 321 (1997).

⁷A. Imhof and D.J. Pine, Nature (London) **389**, 948 (1997).

⁸B.T. Holland, C.F. Blanford, and A. Stein, Science **281**, 538 (1998).

⁹A. Blanco *et al.*, Nature (London) **405**, 437 (2000).

¹⁰H.T. Miyazaki, H. Miyazaki, K. Ohtaka, and T. Sato, J. Appl. Phys. **87**, 7152 (2000).

¹¹M. van Exter and D. Grischkowsky, Phys. Rev. B **41**, 12 140 (1990).

¹²D.H. Auston, K.P. Cheung, and P.R. Smith, Appl. Phys. Lett. **45**, 284 (1984).

¹³M. Tani, S. Matsuura, and K. Sakai, Appl. Opt. **36**, 7853 (1997).

¹⁴K. Ohtaka *et al.*, Phys. Rev. B **61**, 5267 (2000).

¹⁵U. Fano, Phys. Rev. **124**, 1866 (1961).

¹⁶To fit the refractive index $n(\omega) - i\kappa(\omega)$ of Si_3N_4 , we use the

formula $n(f) = 58.3f^3 - 26.2f^2 + 3.50f + 2.85$ and $\kappa(f) = 1.95f^3 - 0.848f^2 + 0.125f - 0.000562$, where $f = \omega/2\pi$ is a frequency in units of THz.

¹⁷M. Hase *et al.*, in *Proceedings of Smart Structures and Materials 2000, Newport Beach, 2000*, edited by V. K. Varadan (SPIE, Washington, 2000), p. 314.

¹⁸Usually, the phase shift spectrum has an uncertainty in the j number in Eq. (4). In order to compare the measured data with the calculated data clearly, the phase shift spectra in Fig. 3 are obtained by determining the j number on the assumption: the phase shift $\Delta\phi(\omega)$ does not change over 2π when $\Delta\phi_0(\omega)$ is a discontinuous function of ω .

¹⁹The Fano effect (Ref. 15) is involved in light transmission because the photonic bands in a 2D or slab system are embedded in the continuum of free-space modes, and coupling takes place between them.

²⁰K. Ohtaka and Y. Tanabe, J. Phys. Soc. Jpn. **65**, 2670 (1996).

²¹K. Sakoda, *Optical Properties of Photonic Crystals* (Springer, Berlin, 2001).

²²K. Ohtaka, J. Lightwave Technol. **17**, 2161 (1999).

²³H. Miyazaki and K. Ohtaka, Phys. Rev. B **58**, 6920 (1998).

²⁴K. Ohtaka and S. Yamaguti, Opt. Quantum Electron. **34**, 235 (2002).